Hindawi Publishing Corporation
International Journal of Reconfigurable Computing
Volume 2012, Article ID 201378, 19 pages
doi:10.1155/2012/201378

Research Article

A Protein Sequence Analysis Hardware Accelerator Based on Divergences

Juan Fernando Eusse,[1] Nahri Moreano,[2] Alba Cristina Magalhaes Alves de Melo,[3] and Ricardo Pezzuol Jacobi[4]

[1] *Electrical Engineering Department, University of Brasilia, Brasilia, DF 70910-900, Brazil*
[2] *School of Computing, Federal University of Mato Grosso do Sul, Campo Grande, MS 79070-900, Brazil*
[3] *Computer Science Department, University of Brasilia, Brasilia, DF 70910-900, Brazil*
[4] *UnB Gama School, University of Brasilia, Gama, DF 72405-610, Brazil*

Correspondence should be addressed to Ricardo Pezzuol Jacobi, jacobi@unb.br

Received 27 September 2011; Accepted 26 December 2011

Academic Editor: Khaled Benkrid

The Viterbi algorithm is one of the most used dynamic programming algorithms for protein comparison and identification, based on hidden markov Models (HMMs). Most of the works in the literature focus on the implementation of hardware accelerators that act as a prefilter stage in the comparison process. This stage discards poorly aligned sequences with a low similarity score and forwards sequences with good similarity scores to software, where they are reprocessed to generate the sequence alignment. In order to reduce the software reprocessing time, this work proposes a hardware accelerator for the Viterbi algorithm which includes the concept of divergence, in which the region of interest of the dynamic programming matrices is delimited. We obtained gains of up to 182x when compared to unaccelerated software. The performance measurement methodology adopted in this work takes into account not only the acceleration achieved by the hardware but also the reprocessing software stage required to generate the alignment.

1. Introduction

Protein sequence comparison and analysis is a repetitive task in the field of molecular biology, as is needed by biologists to predict or determine the function, structure, and evolutional characteristics of newly discovered protein sequences. During the last decade, technological advances had made possible the identification of a vast number of new proteins that have been introduced to the existing protein databases [1, 2]. With the exponential growth of these databases, the execution times of the protein comparison algorithms also grew exponentially [3], and the necessity to accelerate the existing software rose in order to speed up research.

The HMMER 2.3.2 program suite [4] is one of the most used programs for sequence comparison. HMMER takes multiple sequence alignments of similar protein sequences grouped into protein families and builds hidden Markov models (HMMs) [5] of them. This is done to estimate statistically the evolutionary relations that exist between different members of the protein family, and to ease the identification of new family members with a similar structure or function. HMMER then takes unclassified input sequences and compares them against the generated HMMs of protein families (profile HMM) via the Viterbi algorithm (see Section 2), to generate both a similarity score and an alignment for the input (query) sequences.

As the Viterbi routine is the most time consuming part of the HMMER programs, multiple attempts to optimize and accelerate it have been made. MPI-HMMER [6] explores parallel execution in a cluster as well as software optimizations via the Intel-SSE2 instruction set. Other approaches like SledgeHMMER [7] and "HMMER on the Sun Grid" [8] provide web-based search interfaces to either an optimized version of HMMER running on a web server or the Sun Grid, respectively. Other approaches such as ClawHMMER [9] and GPU-HMMER [10] implement GPU parallelization

of the Viterbi algorithm, while achieving a better cost/benefit relation than the cluster approach.

Studies have also shown that most of the processing time of the HMMER software is spent into processing poor scoring (nonsignificant) sequences [11], and most authors have found useful to apply a first-phase filter in order to discard poor scoring sequences prior to full processing. Some works apply heuristics [12], but the mainstream focuses on the use of FPGA-based accelerators [3, 11, 13–16] as a first-phase filter. The filter retrieves the sequence's similarity score and, if it is acceptable, instructs the software to reprocess the sequence in order to generate the corresponding alignment.

Our work proposes further acceleration of the algorithm by using the concept of divergence in which full reprocessing of the sequence after the FPGA accelerator is not needed, since the alignment only appears in specific parts of both the profile HMM model and the sequence. The proposed accelerator outputs the similarity score and the limits of the area of the dynamic programming (DP) matrices that contains the optimal alignment. The software then calculates only that small area of the DP matrices for the Viterbi algorithm and returns the same alignment as the unaccelerated software.

The main contributions of this work are threefold. First, we propose the Plan7-Viterbi divergence algorithm, which calculates the area in the Plan7-Viterbi dynamic programming matrices that contains the sequence-profile alignment. Second, we propose an architecture that implements this algorithm in hardware. Our architecture not only is able to generate the score for a query sequence when compared to a given profile HMM but also generates the divergence algorithm coefficients in hardware, which helps to speed up the subsequent alignment generation process by software. To the best of our knowledge, there is no software adaptation of the divergence algorithm to the Viterbi-Plan7 algorithm nor a hardware implementation of that adaptation. Finally, we propose a new measurement strategy that takes into account not only the architecture's throughput but also reprocessing times. This strategy helps us to give a more realistic measure of the achieved gains when including a hardware accelerator into the HMMER programs.

This work is organized as follows. In Section 2 we clarify some of the concepts of protein sequences, protein families, and profile HMMs. In Section 3 we present the related work in FPGA-based HMMER accelerators. Section 4 introduces the concept of divergences and their use in the acceleration of the Viterbi algorithm. Section 5 shows the proposed hardware architecture. Section 6 presents the metrics used to analyze the performance of the system. In Section 7 we show implementation and performance results, and we compare them with the existing works. Finally, in Section 8 we summarize the results and suggest future works.

2. Protein Sequence Comparison

2.1. Protein Sequences, Protein Families, and Profile HMMs. Proteins are basic elements that are present in every living organism. They may have several important functions such as catalyzing chemical reactions and signaling if a gene must be expressed, among others. Essentially, a protein is a chain of amino acids. In the nature, there are 20 different amino acids, represented by the alphabet $\Sigma = \{A, C, D, E, F, G, H, I, K, L, M, N, P, Q, R, S, T, V, W, Y\}$ [17].

A protein family is defined to be a set of proteins that have similar function, have similar 2D/3D structure, or have a common evolutionary history [17]. Therefore, a newly sequenced protein is often compared to several known protein families, in search of similarities. This comparison usually aligns the protein sequence to the representation of a protein family. This representation can be a profile, a consensus sequence, or a signature [18]. In this paper, we will only deal with profile representations, which are based on multiple sequence alignments.

Given a multiple-sequence alignment, a profile specifies, for each column, the frequency that each amino acid appears in the column. If a sequence-profile comparison results in high similarity, the protein sequence is usually identified to be a member of the family. This identification is a very important step towards determining the function and/or structure of a protein sequence.

One of the most accepted probabilistic models to do sequence-profile comparisons is based on hidden Markov models (HMMs). It is called profile HMM because it groups the evolutionary statistics for all the family members, therefore "profiling" it. A profile HMM models the common similarities among all the sequences in a protein family as discrete states; each one corresponding to an evolutionary possibility such as amino acid insertions, deletions, or matches between them. The traditional profile HMM architecture proposed by Durbin et al. [5] consisted of insert (I), delete (D), and match (M) states.

The HMMER suite [4], is a widely used software implementation of profile HMMs for biological sequence analysis, composed of several programs. In particular, the program *hmmsearch* searches a sequence database for matches to an HMM, while the program *hmmpfam* searches an HMM database for matches to a query sequence.

HMMER uses a modified HMM architecture that in addition to the traditional *M, I*, and *D* states includes flanking states that enable the algorithm to produce global or local alignments, with respect to the model or to the sequence, and also multiple-hit alignments [4, 5]. The Plan7 architecture used by HMMER is shown in Figure 1. Usually, there is one match state for each consensus column in the multiple alignment. Each M state aligns to (emits) a single residue, with a probability score that is determined by the frequency in which the residues have been observed in the corresponding column of the multiple alignment. Therefore, each M state has 20 probabilities for scoring the 20 amino acids.

The insertion (I) and deletion (D) states model gapped alignments, that is, alignments including residue insertions and deletions. Each I state also has 20 probabilities for scoring the 20 amino acids. The group of *M, I*, and *D* states corresponding to the same position in the multiple alignment is called a node of the HMM. Beside the emission

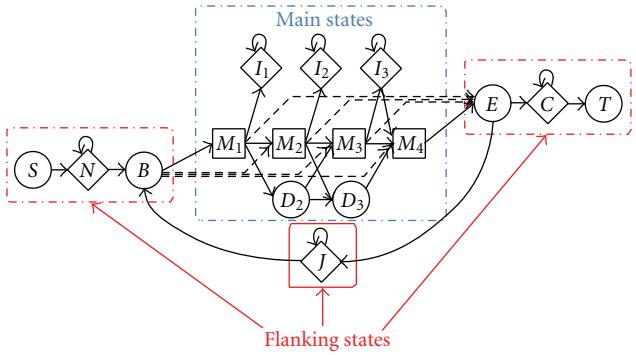

Figure 1: Plan7 architecture used by HMMER [3].

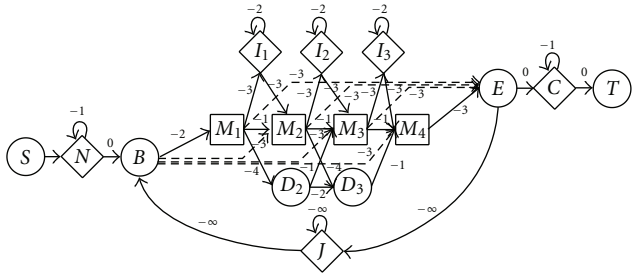

Figure 2: A profile HMM with 4 nodes and the transition scores.

probabilities, there are transition probabilities associated to each transition from one state to another.

2.2. Viterbi Algorithm. Given a HMM modeling a protein family and a query sequence, HMMER computes the probability that the sequence belongs to the family, as a similarity score, and generates the resulting alignment if the score is sufficiently good. To do so, it implements a well-known DP algorithm called the Viterbi algorithm [19]. This algorithm calculates a set of score matrices (corresponding to states *M*, *I*, and *D*) and vectors (corresponding to states *N*, *B*, *E*, *C*, and *J*) by means of a set of recurrence equations. As a result, it finds the best (most probable) alignment and its score for the query sequence with the given model.

Equations (1) show the Viterbi algorithm recurrence relations for aligning a sequence of length n to a profile HMM with k nodes. In these equations, $M(i, j)$ is the score of the best path aligning the subsequence $s_1 \ldots s_i$ to the submodel up to state M_j and $I(i, j)$ and $D(i, j)$ are defined similarly. The emission probability of the amino acid s_i at state$_1$ is denoted by em(state$_1$,s_i), while tr(state$_1$,state$_2$) represents the transition cost from state$_1$ to state$_2$. The similarity score of the best alignment is given by $C(n) + \mathrm{tr}(C, T)$.

Plan7-Viterbi algorithm recurrence equations, for a profile HMM with k nodes and sequence s of length n are as follows;

$$M(i,0) = I(i,0) = D(i,0) = -\infty \quad \forall 1 \le i \le n,$$

$$M(0,j) = I(0,j) = D(0,j) = -\infty \quad \forall 0 \le j \le k,$$

$$M(i,j) = \mathrm{em}\left(M_j, s_i\right) + \max\begin{cases} M(i-1,j-1) + \mathrm{tr}\left(M_{j-1}, M_j\right) \\ I(i-1,j-1) + \mathrm{tr}\left(I_{j-1}, M_j\right) \\ D(i-1,j-1) + \mathrm{tr}\left(D_{j-1}, M_j\right) \\ B(i-1) + \mathrm{tr}\left(B, M_j\right) \end{cases} \quad \forall 1 \le i \le n,$$

$$I(i,j) = \mathrm{em}\left(I_j, s_i\right) + \max\begin{cases} M(i-1,j) + \mathrm{tr}\left(M_j, I_j\right) \\ I(i-1,j) + \mathrm{tr}\left(I_j, I_j\right) \end{cases} \quad \forall 1 \le j \le k,$$

$$D(i,j) = \max\begin{cases} M(i,j-1) + \mathrm{tr}\left(M_{j-1}, D_j\right) \\ D(i,j-1) + \mathrm{tr}\left(D_{j-1}, D_j\right), \end{cases}$$

$$N(0) = 0,$$

$$N(i) = N(i-1) + \mathrm{tr}(N,N), \quad \forall 1 \le i \le n,$$

$$B(0) = \mathrm{tr}(N,B),$$

$$B(i) = \max\begin{cases} N(i) + \mathrm{tr}(N,B) \\ J(i) + \mathrm{tr}(J,B) \end{cases} \quad \forall 1 \le i \le n,$$

$$E(i) = \max_{1 \le j \le k} \left(M(i,j) + \mathrm{tr}\left(M_j, E\right)\right) \quad \forall 1 \le j \le k,$$

$$J(0) = -\infty,$$

$$J(i) = \max\begin{cases} J(i-1) + \mathrm{tr}(J,J) \\ E(i) + \mathrm{tr}(E,J) \end{cases} \quad \forall 1 \le i \le n,$$

$$C(0) = -\infty,$$

$$C(i) = \max\begin{cases} C(i-1) + \mathrm{tr}(C,C) \\ E(i) + \mathrm{tr}(E,C) \end{cases} \quad \forall 1 \le i \le n.$$

$$\text{similarity\_score} = C(n) + \mathrm{tr}(C,T). \tag{1}$$

Figure 2 illustrates a profile HMM with 4 nodes representing a multiple-sequence alignment. The transition scores are shown in the figure, labeling the state transitions. The emission scores for the M and I states are shown in Table 1.

Table 2 shows the score matrices and vectors computed by the Viterbi algorithm, while aligning the query sequence ACYDE to the profile HMM given in Figure 2. The best alignment has the similarity score of 25 and corresponds to

Table 1: Emission scores of amino acids for match and insert states of profile HMM of Figure 2.

State	A	C	D	E	F, I, L, M, V, W	G, K, P, S	H, Q, R, T	Y
M_1	7	−1	−1	1	−1	2	1	−1
M_2	−1	9	−1	1	−1	2	1	−1
M_3	−1	−1	8	2	−1	2	1	−1
M_4	−1	−1	3	9	−1	2	1	−1
I_1	−1	−1	0	1	−1	0	1	2
I_2	−1	−1	0	1	−1	0	1	2
I_3	−1	−1	0	1	−1	0	1	2

Table 2: Score matrices and vectors of the Viterbi algorithm for the comparison of the sequence ACYDE against the profile HMM of Figure 2.

	N	B	M					I					D					E	J	C
			0	1	2	3	4	0	1	2	3	4	0	1	2	3	4			
—	0	0	−∞	−∞	−∞	−∞	−∞	−∞	−∞	−∞	−∞	−∞	−∞	−∞	−∞	−∞	−∞	−∞	−∞	−∞
A	−1	−1	−∞	−5	−4	−4	−4	−∞	−∞	−∞	−∞	−∞	−∞	−∞	1	−1	−3	2	−∞	2
C	−2	−2	−∞	−4	13	−1	−3	−∞	1	−8	−8	−8	−∞	−∞	−8	9	7	10	−∞	10
Y	−3	−3	−∞	−5	−3	11	7	−∞	1	12	2	−4	−∞	−∞	−9	−7	7	8	−∞	9
D	−4	−4	−∞	−6	−3	17	13	−∞	−1	10	8	6	−∞	−∞	−10	−7	13	14	−∞	14
E	−5	−5	−∞	−5	−3	9	25	−∞	−2	9	15	24	−∞	−∞	−9	−7	5	25	−∞	25

the path $(S,\text{-}) \rightarrow (N,\text{-}) \rightarrow (B,\text{-}) \rightarrow (M1,A) \rightarrow (M2,C) \rightarrow (I2,Y) \rightarrow (M3,D) \rightarrow (M4,E) \rightarrow (E,\text{-}) \rightarrow (C,\text{-}) \rightarrow (T,\text{-})$.

3. Related Work

The function that implements the Viterbi algorithm in the HMMER suite is the most time consuming of the *hmmsearch* and *hmmpfam* programs of the suite. Therefore, most works [3, 11, 13–16, 20] focus on accelerating its execution by proposing a pre-filter phase which only calculates the similarity score for the algorithm. Then, if the similarity score is good, the entire query sequence is reprocessed to produce the alignment.

In general, FPGA-based accelerators for the Viterbi algorithm are composed of processing elements (PEs), connected together in a systolic array to exploit parallelism by eliminating the J state of the Plan7 Viterbi algorithm (Section 2.2). Usually, each node in the profile HMM is implemented by one PE. However, since the typical profile HMMs contain more than 600 nodes, even the recent FPGAs cannot accommodate this huge number of processing elements. For this reason, the entire sequence processing is divided into several passes [3, 11, 13, 14].

First-in first-out memories are included inside the FPGA implementation to store the necessary intermediary data between passes. Transition and emission probabilities for all the passes of the HMM are preloaded into block memories inside the FPGA to hide model turn around (transition probabilities reloading) when switching between passes. These memory requirements impose restrictions on the maximum PE number that can fit into the device, the maximum HMM size, and the maximum sequence size.

Benkrid et al. [13] propose an array of 90 PEs, capable of comparing a 1024 element sequence with a profile HMM containing 1440 nodes. They eliminate the J state dependencies in order to exploit the dynamic programming parallelism and calculate one cell element per clock cycle in each PE, reporting a maximum performance of 9 GCUPS (giga cell updates per second). Their systolic array was synthesized into a Virtex 2 Pro FPGA with a 100 MHz clock frequency.

Maddimsetty et al. [11] enhance accuracy by reducing the precision error induced by the elimination of the J state and proposes a two-pass architecture to detect and correct false negatives. Based on technology assumptions, they report an estimated maximum size of 50 PEs at an estimated clock frequency of 200 MHz and supposing a performance of 5 to 20 GCUPS.

Jacob et al. [3] divide the PE into 4 pipeline stages, in order to increase the maximum clock frequency up to 180 MHz and the throughput up to 10 GCUPS. Their work also eliminates the J state. The proposed architecture was implemented in a Xilinx Virtex 2 6000 and supports up to 68 PEs, a HMM with maximum length of 544 nodes, and a maximum sequence size of 1024 amino acids.

In Derrien and Quinton [16], a methodology to implement a pipeline inside the PE is outlined, based on the mathematical representation of the algorithm. Then a design space exploration is made for a Xilinx Spartan 3 4000, with maximum PE clock frequency of 66 MHz and a maximum performance of about 1.3 GCUPS.

Oliver et al. [14] implement the typical PE array without taking into account the J state when calculating the score. They obtain an array of 72 PEs working at a clock rate of 74 MHz, and an estimated performance of 3.95 GCUPS.

In [20] a special functional unit is introduced to detect when the J state feedback loop is taken. Then a control unit updates the value for state B and instructs the PEs to

recalculate the inaccurate values. The implementation was made in a Xilinx Virtex 5 110-T FPGA with a maximum of 25 PEs and operating at 130 MHz. The reported performance is 3.2 GCUPS. No maximum HMM length or pass number is reported in the paper.

Takagi and Maruyama [21] developed a similar solution for processing the feedback loop. The alignment is calculated speculatively in parallel, and, when the feedback loop is taken, the alignment is recalculated from the beginning using the feedback score. With a Xilinx XC4VLX160 they could implement 100 PEs for profiles not exceeding 2048 nodes, reaching speedups up to 360 when compared to an Intel Core 2 Duo, 3.16 Ghz, and 4 GB RAM, when no recalculation occurs, and with a corresponding speed-up reduction otherwise.

Walters et al. [15] implement a complete Plan7-Viterbi algorithm in hardware, by exploiting the inherent parallelism in processing different sequences against the same HMM at the same time. Their PE is slightly more complex than those of other works as it includes the *J* state in the score calculation process. They include hardware acceleration into a cluster of computers, in order to further enhance the speedup. The implementation was made in a Xilinx Spartan 3 1500 board with a maximum of 10 PEs per node and a maximum profile HMM length of 256. The maximum clock speed for each PE is 70 MHz, and the complete system yields a performance of 700 MCUPS per cluster node, in a cluster comprised of 10 worker nodes. As any of the other analyzed works, its only output is the sequence score, and for the trace back, a complete reprocessing of the sequence has to be done in software.

Like all the designs discussed in this section, our design does not calculate the alignment in hardware, providing the score as output. Nevertheless, unlike the previous FPGA proposals, our design also provides information that can be used by the software to significantly reduce the number of cells contained in the DP matrices that need to be recalculated. Therefore, beside the score, our design outputs also the divergence algorithm information that will be used by the software to determine a region in the DP matrices where the actual alignment occurs. In this way, the software reprocessing time can be reduced, and better overall speedups can be attained.

Our work also proposes the use of a more accurate performance measurement that includes not only the time spent calculating the sequence score and divergence but also the time spent while reprocessing the sequences of interest, which gives a clearer idea of the real gain achieved when integrating the accelerator to HMMER.

4. Plan7-Viterbi Divergence Algorithm

The divergence concept was first introduced by Batista et al. [22], and it was included into an exact variation of the Smith-Waterman algorithm for pairwise local alignment of DNA sequences. Their goal was to obtain the alignment of huge biological sequences, handling the quadratic space, and time complexity of the Smith-Waterman algorithm. Therefore, they used parallel processing in a cluster of processors to reduce execution time and exploited the divergence concept to reduce memory requirements. Initially, the whole similarity matrix is calculated in linear space. This phase of the algorithm outputs the highest similarity score and the coordinates in the similarity matrix that define the area that contains the optimal alignment. These coordinates were called superior and inferior divergences. To obtain the alignment itself using limited memory space, they recalculate the similarity matrix, but this time only the cells inside the limited area need to be computed and stored.

A direct adaptation of the original divergence concept to the Plan7-Viterbi algorithm is not possible because the recurrence relations of the Smith-Waterman and Plan7-Viterbi are totally distinct. The Smith-Waterman algorithm with affine gap calculates three DP matrices (*E*, *F*, *D*), but the inferior and superior divergence could be inferred from only one matrix (*D*) [22]. In the Plan7-Viterbi algorithm (Section 2.2), the inferior and superior divergence information depend on matrices *M*, *I*, *D* and vectors *C*, *E*. For this reason, we had to generate entirely new recurrence relations for divergence calculation. This resulted in a new algorithm, which we called the Plan7-Viterbi divergence algorithm. The recurrence equations for the *M* State of the proposed algorithm are shown in (3) and (4).

Also, the Smith-Waterman divergence algorithm provides a band in the DP matrix, where the alignment occurs, which is limited by the superior and inferior divergences [22]. We observed that the alignment region could be further limited if the initial and final rows are provided, in addition to the superior and inferior divergence information. Therefore, we also extended the divergence concept to provide a polygon that encapsulates the alignment, instead of two parallel lines, as it was defined in the Smith-Waterman divergence algorithm [22]. In the following paragraphs, we describe the Plan7-Viterbi divergence algorithm.

Given the DP matrices of the Viterbi algorithm, the limits of the best alignment are expressed by its initial and final rows and superior and inferior divergences (IR, FR, SD, and ID, resp.). The initial and final rows indicate the row of the matrices where the alignment starts and ends (initial and final element of the sequence involved in the alignment). The superior and inferior divergences represent how far the alignment departs from the main diagonal, in up and down directions, respectively. The main diagonal has divergence 0, the diagonal immediately above it has divergence -1, the next one -2, and so on. Analogously, the diagonals below the main diagonal have divergences $+1$, $+2$, and so on. These divergences are calculated as the difference $i - j$ between the row (i) and column (j) coordinates of the matrix cell. Figure 3 shows the main ideas behind the Plan7-Viterbi divergence algorithm.

Given a profile HMM with k nodes and a query sequence of length n, the figure shows the DP matrices *M*, *I*, *D* (represented as only one matrix, for clarity) of the Viterbi algorithm. The best alignment of the sequence to the HMM is a path (shown in a thick line) along the cells of the matrices. The initial and final rows of the alignment are 3 and 7, respectively, while the alignment superior and inferior divergences are -3 and 0, respectively. These limits

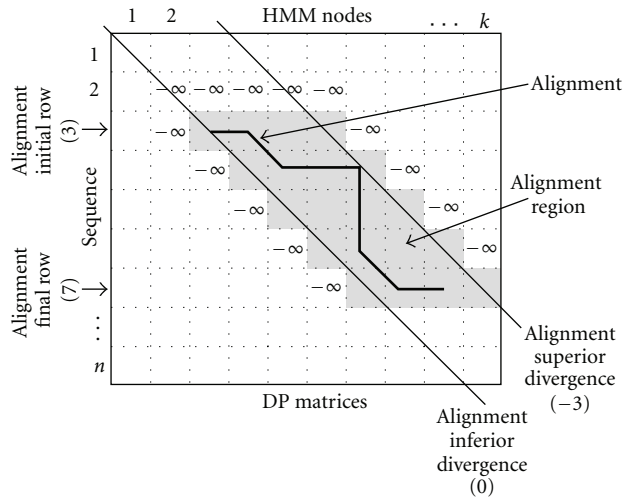

Figure 3: Divergence concept: alignment limits, initialized cells (with $-\infty$), and alignment region, for a HMM with k nodes and a sequence of length n.

determine what we define as the alignment region (AR), shown in shadow in the figure.

The AR contains the cells of the score matrices M, I, and D that must be computed in order to obtain the best alignment. The other Viterbi algorithm DP vectors are also limited by IR and FR, as well. The alignment limits are calculated precisely, leaving no space to error, in a sense that computing only the cells inside the AR will produce the same best alignment as the unbounded (not limited to the AR) computation of the whole matrices.

The Plan7-Viterbi Divergence Algorithm (Plan7-Viterbi-DA) works in two main phases. The first phase is inserted into a simplified version of the Viterbi algorithm which eliminates data dependencies induced by the J state. In this phase, we compute the similarity score of the best alignment of the sequence against the profile HMM, but we do not obtain the alignment itself. We also calculate the limits of the alignment, while computing the similarity score. These limits are computed as new DP matrices and vectors, by means of a new set of recurrence equations. The alignment limits IR, SD, and ID are computed for the *M, I, D, E,* and *C* states. The FR limit is computed only for the *C* state.

The Viterbi algorithm in (1) has the recurrence equation (2) for the M state score computation:

$$M(i,j) = \mathrm{em}\left(M_j, s_i\right) + \max\begin{cases} M(i-1,j-1) + \mathrm{tr}\left(M_{j-1}, M_j\right) \\ I(i-1,j-1) + \mathrm{tr}\left(I_{j-1}, M_j\right) \\ D(i-1,j-1) + \mathrm{tr}\left(D_{j-1}, M_j\right) \\ B(i-1) + \mathrm{tr}\left(B_{i-1}, M_j\right). \end{cases} \quad (2)$$

Let Sel_M assume the values 0, 1, 2 or 3, depending on the result of the maximum operator in (2). If the argument selected by the maximum operator is the first, second, third, or fourth one, then Sel_M will assume the value 0, 1, 2, or 3, respectively. Then, the alignment limits IR, SD, and ID, concerning the score matrix M, are defined by the recurrence equations in (6).

Recurrence equations for the alignment limits IR, SD, and ID, concerning the score matrix M, for $1 \le i \le n$ and $1 \le j \le k$:

$$\mathrm{IR}_M(i,j) = \begin{cases} \mathrm{IR}_M(i-1,j-1), & \text{if } \mathrm{Sel}_M = 0 \\ \mathrm{IR}_I(i-1,j-1), & \text{if } \mathrm{Sel}_M = 1 \\ \mathrm{IR}_D(i-1,j-1), & \text{if } \mathrm{Sel}_M = 2 \\ i, & \text{if } \mathrm{Sel}_M = 3, \end{cases}$$

$$\mathrm{SD}_M(i,j) = \begin{cases} \mathrm{SD}_M(i-1,j-1), & \text{if } \mathrm{Sel}_M = 0 \\ \min(i-j, \mathrm{SD}_I(i-1,j-1)), & \text{if } \mathrm{Sel}_M = 1 \\ \min(i-j, \mathrm{SD}_D(i-1,j-1)), & \text{if } \mathrm{Sel}_M = 2 \\ i-j, & \text{if } \mathrm{Sel}_M = 3, \end{cases}$$

$$\mathrm{ID}_M(i,j) = \begin{cases} \mathrm{ID}_M(i-1,j-1), & \text{if } \mathrm{Sel}_M = 0 \\ \max(i-j, \mathrm{ID}_I(i-1,j-1)), & \text{if } \mathrm{Sel}_M = 1 \\ \max(i-j, \mathrm{ID}_D(i-1,j-1)), & \text{if } \mathrm{Sel}_M = 2 \\ i-j, & \text{if } \mathrm{Sel}_M = 3. \end{cases} \quad (3)$$

The alignment limits IR, SD, and ID, related to the score matrices I and D and vector E, are defined analogously, based on the value of Sel_I, Sel_D, and Sel_E, determined by the result of the maximum operator of the Viterbi algorithm recurrence equation for the I, D, and E states, respectively. Given the recurrence equation for the C state's score computation in the Viterbi algorithm in (1), let Sel_C assume the values 0 or 1, depending on the result of the maximum operator in this equation. Equation (4) shows the recurrence equations that define the alignment limits IR, FR, SD, and ID, concerning the C score vector.

The first phase of the Plan7-Viterbi-DA was thought to be implemented in hardware because its implementation in software would increase the memory requirements and processing time as it introduces new DP matrices. Besides, the Divergence values computation does not create new data dependencies inside the Viterbi algorithm and can be performed in parallel to the similarity score calculation.

The second phase of the Plan7-Viterbi-DA uses the output data coming from the first one (similarity score and divergence values). If the alignment's similarity score is significant enough, then the second phase generates the alignment. To do this the software executes the Viterbi algorithm again for that sequence.

Nevertheless, it is not necessary to compute the whole DP matrices of the Viterbi algorithm, as we use the alignment limits produced by the first phase in order to calculate only the cells inside the AR of the DP matrices, thus saving memory space and execution time. Figure 4 illustrates

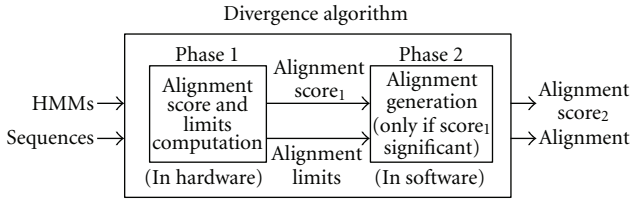

Figure 4: Phases of the Plan7-Viterbi-DA.

the high-level structure of the Plan7-Viterbi-DA and the interaction between its two phases.

Recurrence equations for the alignment limits IR, FR, SD, and ID, concerning the C score vector, for $1 \le i \le n$:

$$\begin{aligned}
\mathrm{IR}_C(i) &= \begin{cases} \mathrm{IR}_C(i-1), & \text{if } \mathrm{Sel}_C = 0 \\ \mathrm{IR}_E(i), & \text{if } \mathrm{Sel}_C = 1, \end{cases} \\
\mathrm{FR}_C(i) &= \begin{cases} \mathrm{FR}_C(i-1), & \text{if } \mathrm{Sel}_C = 0 \\ i, & \text{if } \mathrm{Sel}_C = 1, \end{cases} \\
\mathrm{SD}_C(i) &= \begin{cases} \mathrm{SD}_C(i-1), & \text{if } \mathrm{Sel}_C = 0 \\ \mathrm{SD}_E(i), & \text{if } \mathrm{Sel}_C = 1, \end{cases} \\
\mathrm{ID}_C(i) &= \begin{cases} \mathrm{ID}_C(i-1), & \text{if } \mathrm{Sel}_C = 0 \\ \mathrm{ID}_E(i), & \text{if } \mathrm{Sel}_C = 1. \end{cases}
\end{aligned} \tag{4}$$

The Plan7-Viterbi-DA's second phase is implemented in software as a modification inside HMMER's Viterbi function used by the *hmmpfam* and *hmmsearch* programs. In this function, we need to initialize with $-\infty$ only the cells immediately above, to the left and to the right of the AR, as shown in Figure 3. The main loops are also modified in order to calculate only the cells inside the AR, using the alignment limits IR, FR, SD, and ID.

In the next section we propose a hardware implementation of the first phase of Plan7-Viterbi-DA.

5. HMMER-ViTDiV Architecture

The proposed architecture, called HMMER-ViTDiV, consists of an array of interconnected processing elements (PEs) that implements a simplified version of the Viterbi algorithm, including the necessary modifications to calculate the Plan7-Viterbi-DA presented in Section 4. The architecture is designed to be integrated to the system as a pre-filter stage that returns the similarity score and the alignment limits for a query sequence with a specific profile HMM. If the similarity score for the query sequence is significant enough, then the software uses the alignment limits calculated for the sequence inside the architecture and generates the alignment using the Plan7-Viterbi-DA. Each PE calculates the score for the j column of the DP matrices of the Viterbi algorithm and the alignment limits for the same column. Figure 5 shows the DP matrices antidiagonals and their relationship with each one of the PEs when the number of profile HMM nodes is equal

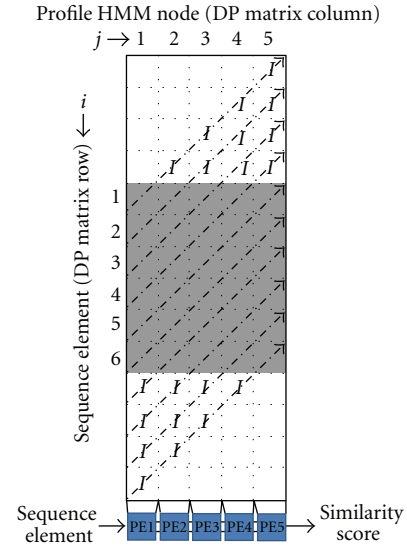

Figure 5: PE to DP matrices correspondence when the HMM number of nodes is less or equal to the number of PEs.

to the number of implemented PEs inside the architecture. In the figure, the arrows show the DP matrices anti-diagonals, cells marked with I correspond to idle PEs, and shaded cells correspond to DP cells that are being calculated by their corresponding PE. The systolic array is filled gradually as the sequence elements are inserted until there are no idle PEs left, and then, when sequence elements are exiting, it empties until there are no more DP cells to calculate.

Since the size of commercial FPGAs is currently limited, today we cannot implement a system with a number of PEs that is equal to one of the largest profile HMM in sequence databases (2295) [2]. We implemented a system that divides the computation into various passes, each one computing a band of size N of the DP matrices, where N is the maximum number of PEs that fits into the target FPGA. In each pass the entire sequence is fed across the array of PEs and the scores are calculated for the current band. Then the output of the last PE of the array is stored inside FIFOs, as it is the input to the next pass and will be consumed by the first PE. Figure 6 presents the concept of band division and multiple passes.

As shown in Figure 6, in each pass the PE acts as a different node of the profile HMM and has to be loaded with the corresponding transition and emission probabilities that are required by the calculations. Also, we note that the system does not have to wait for the entire sequence to be out of the array in one pass to start the next pass, and the PEs can be in different passes at a given time.

Two RAM memories per PE are included inside the architecture to store and provide the transition and emission probabilities for all passes. Two special sequence elements are included in the design to ease the identification of the end of a pass (@) and the end of the sequence processing (*). A controller is implemented inside each PE to identify these two characters, increment or clear the pass number, and signal the transition and emission RAM memories as their address offset depends directly on the pass number.

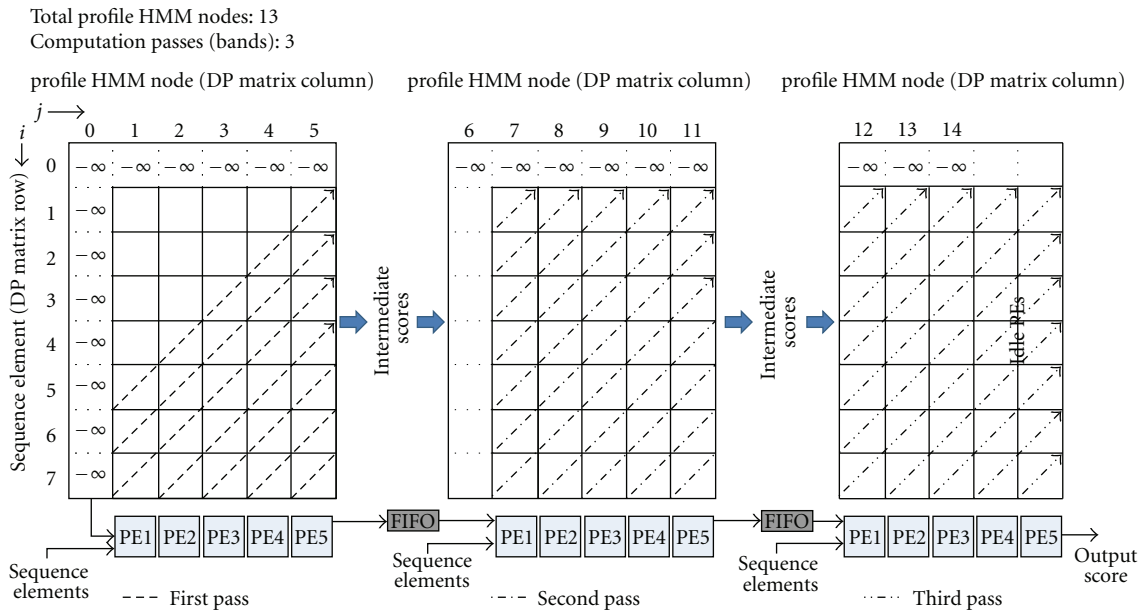

Figure 6: PE to DP matrices correspondence for HMMs with more nodes than the number of PEs (band division and multiple passes).

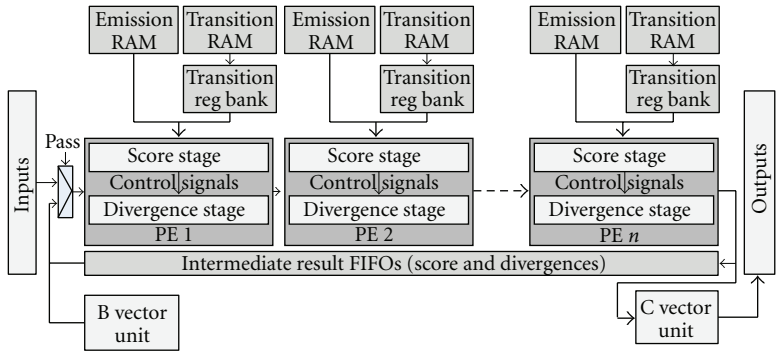

Figure 7: Block diagram of the accelerator architecture.

An input multiplexer had to be included to choose between initialization data for the first pass and intermediate data coming from the FIFOs for the other passes.

A transition register bank had also to be included to store the 9 transition probabilities used concurrently by the PE. This bank is loaded in 5 clock cycles by a small controller inside the transition block RAM memory. Figure 7 shows a general diagram of the architecture.

As illustrated in Figure 7, the PE consists of a score stage which calculates the M, I, D, and E scores and a Plan7-Viterbi divergence stage which calculates the alignment limits for the current sequence. Additional modules are included for the B and C score vector calculations which were placed outside the PE array in order to have an easily modifiable and homogeneous design.

5.1. Score Stage. This stage calculates the scores for the M, I, D, and E states of the simplified Viterbi algorithm (without the J state). Each PE represents an individual HMM node, and calculates the scores as each element of the sequence passes through. The PE's inputs are the scores calculated for the current element in a previous HMM node, and the PE's outputs are the scores for the current sequence element in the current node. The score stage of the PE uses (a) 16-bit saturated adders which detect and avoid overflow or underflow errors by saturating the result either to 32767 or to -32768 and (b) modified maximum units which not only return the maximum of its inputs but also the index of which of them was chosen. Finally, the score stage consists also of 8 16-bit registers used to store the data required by the DP algorithm to calculate the next cell of the matrix. Figure 8 shows the operator diagram of the score stage. The 4-input maximum unit was implemented in parallel in order to reduce the critical path of the system and thus increase the operating frequency.

5.2. Plan7-Viterbi Divergence Stage. This stage calculates the alignment limits for the current query sequence element. The stage inputs are the previous node alignment limits for the current query sequence element, and the outputs are

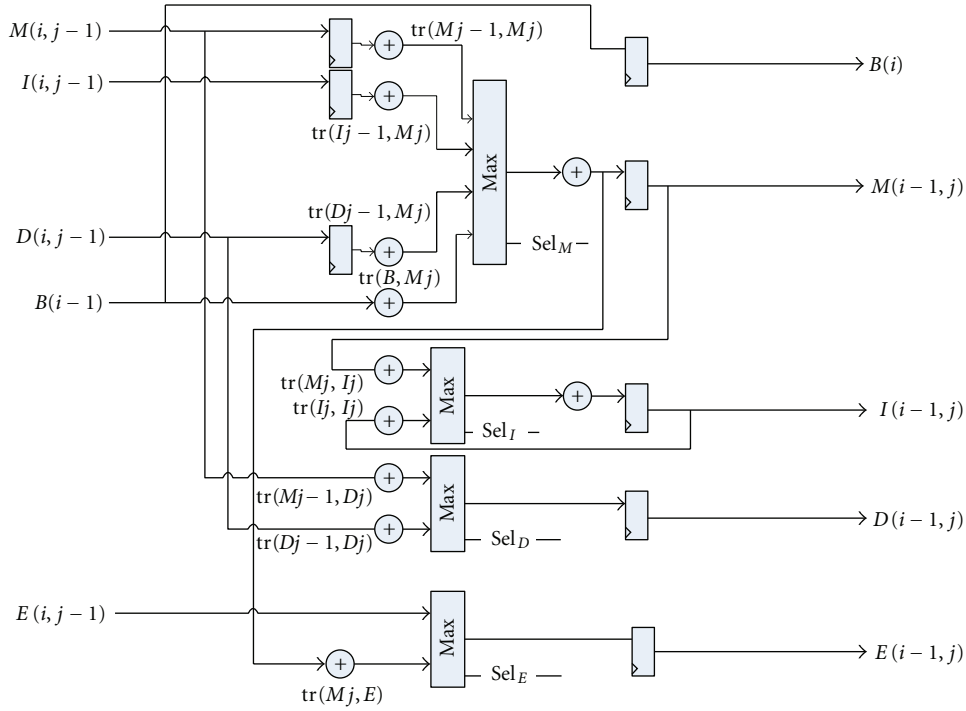

Figure 8: Score stage for the architecture's PE.

the calculated alignment limits for the current element. The outputs depend directly on the score stage of the PE and are controlled by the Sel_M, Sel_I, Sel_D, and Sel_E signals. The divergence stage also requires the current sequence element index, in order to calculate the alignment limits. Figure 9 shows the Plan7-Viterbi-DA implementation for the *M* and *E* states.

Figures 10 and 11 show the Plan7-Viterbi-DA implementation for the *I* and *D* states, respectively. The Base *J* parameter is the position of the PE in the systolic array, and the #PE parameter is the total number of PEs in the current system implementation. These parameters are used to initialize the divergence stage registers according to the current pass and ensure that the limits are calculated correctly. The divergence stage is composed of (a) 2 input maximum and minimum operators, (b) 4 and 2 input multiplexers, in which the selection lines are connected to the control signals coming from the score stage, and (c) 16-bit registers, which serve as temporal storage for the DP data that is needed to calculate the current divergence DP cell.

5.3. B and C Score Vector Calculation Units. The *B* score Vector calculation unit is in charge of feeding the PE array with the *B* score values. This module is placed left of the first PE, and it is connected to the $B(i-1)$ input of it. It has to be initialized for the first iteration with the $\text{tr}(N,B)$ transition probability for the current profile HMM by the control software. For other iterations, it adds the $\text{tr}(N,N)$ probability to the previous values and feeds the output to the first PE. As discussed in Sections 2 and 4, the Plan7-Viterbi-DA does not generate modifications to the *B* calculation unit. Figure 12 shows its hardware implementation.

The *C* calculation unit is in charge of consuming the *E* output provided by the last PE of the array and generating the output similarity score for the current element of the query sequence (the score for the best alignment up to this sequence element). Since the Plan7-Viterbi-DA introduces the calculation of the limits for the best alignment in this state of the Viterbi algorithm, the score stage of the *C* unit also delivers the control signal (Sel_C) for the multiplexers of the divergence stage. Figure 13 shows the *C* state calculation unit, including the score and divergence stages.

6. Proposed Performance Measurement

In order to assess the proposed architecture's performance we used two approaches. The first uses the cell updates per second (CUPS) metric, which is utilized by the majority of the previous works [3, 11, 13–16, 20] and measures the quantity of DP matrix cells that the proposed architecture is capable of calculating in one second. We chose this metric in order to compare the performance of our system to the other proposed accelerators. The weakness of the CUPS approach is that it does not consider the reprocessing time and therefore the alignment generation for unaccelerated software, providing an unrealistic measure of the achieved acceleration when integrating the hardware to HMMER.

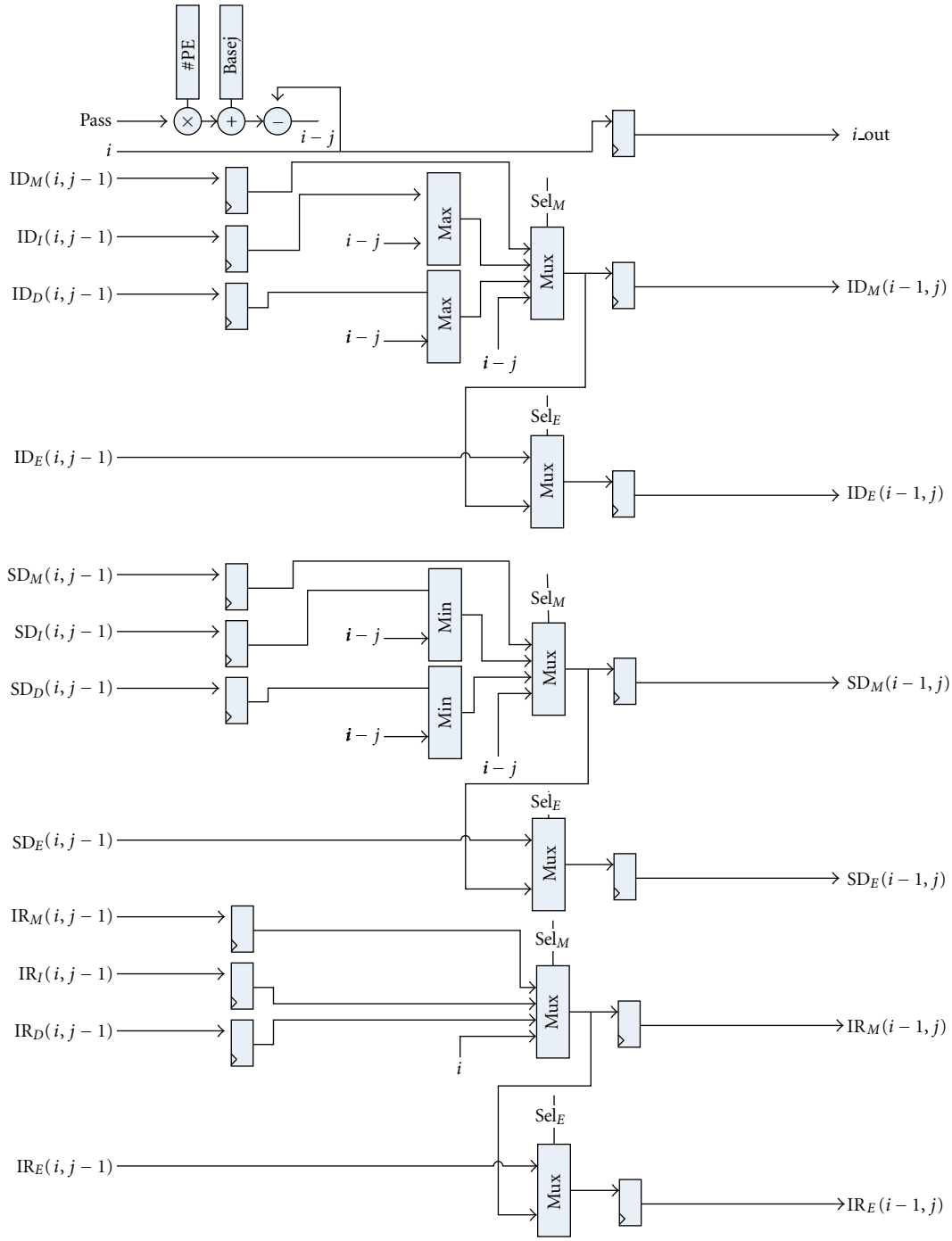

Figure 9: Divergence calculating stage for M and E states.

The second approach measures the execution times of the unaccelerated software when executing a predefined set of sequence comparisons. Then compares it to the execution time of the accelerated system when executing the same set of experiments, to obtain the real gain when integrating a hardware accelerator and the Plan7-Viterbi-DA.

Let S_t be the total number of query sequences in the test set, P_t the total number of profile HMMs in the test set, $t_{s(i,j)}$ the time the unaccelerated *hmmsearch* takes to compare the query sequence S_i to the profile HMM P_j, $t_{\text{rep}(i,j)}$ the time the Plan7-Viterbi-DA takes to reprocess the significant query sequence S_i and the profile HMM P_j, $t_{\text{con}(i,j)}$ the time spent in communication and control tasks inside the accelerated system, and $t_{h(i,j)}$ the time the hardware accelerator takes to execute the comparison between the query sequence S_i and the profile HMM P_j.

Then (5), (6), and (7) show the total time spent by unaccelerated HMMER (T_{ss}), the total time spent by the

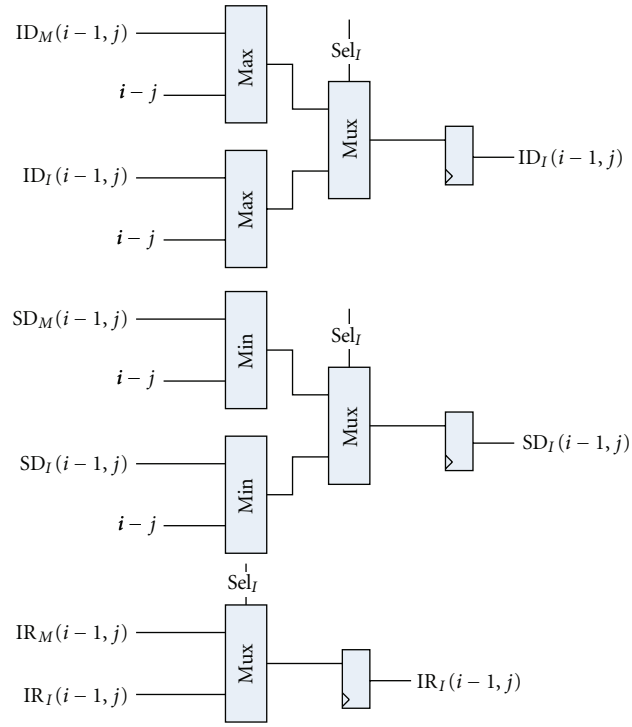

Figure 10: I state divergence calculating stage.

accelerated system (T_{sa}), and the achieved performance gains (G). The times $t_{s(i,j)}$, $t_{h(i,j)}$, $t_{\mathrm{rep}(i,j)}$, and $t_{\mathrm{con}(i,j)}$ are obtained directly from HMMER, the implemented accelerator, and the software implementing the Plan7-Viterbi-DA and will be shown in the following sections:

$$T_{ss} \longleftarrow \sum_{i=1}^{S_t} \sum_{j=1}^{P_t} t_{s(i,j)}, \tag{5}$$

$$T_{sa} \longleftarrow \sum_{i=1}^{S_t} \sum_{j=1}^{P_t} \left(t_{h(i,j)} + t_{\mathrm{rep}(i,j)} + t_{\mathrm{con}(i,j)} \right), \tag{6}$$

$$G \longleftarrow \frac{T_{ss}}{T_{sa}}. \tag{7}$$

7. Experimental Results

The proposed architecture not only enhances software execution by applying a pre-filter to the HMMER software but also provides a means to limit the area of the DP matrices that needs to be reprocessed, by software, in the case of significant sequences. Because of this, the speedup of the solution must be measured by taking into account the performance achieved by the hardware pre-filter as well as the saved software processing time by only recalculating the scores inside the alignment region. Execution time is measured separately for the hardware by measuring its real throughput rate (including loading time and interpass delays) and for software by computing the savings when calculating the scores and the alignment of the divergence-limited region of the DP matrices (Figure 3).

Experimental tests were conducted over all the 10340 profile HMMs for the PFam-A protein database [2]. Searches were made using 4 sets of 2000 randomly sampled protein sequences from the UniProtKB/SwissProt protein database [1] and only significantly scoring sequences were considered to be reprocessed in software. To find out which sequences from the sequence set were significant, we utilized a user-defined threshold and relaxed it to include the greatest possible number of sequences [11]. The experiments were done several times to guarantee the repeatability of them and the stability of the obtained data.

7.1. Implementation and Synthesis Results. The complete system was implemented in VHDL and mapped to an Altera Stratix II EP2S180F1508C3 device. Several configurations were explored to maximize the number of HMM nodes, the number of PEs, and the maximum sequence length. In order to do design space exploration, we developed a parameterizable VHDL code, in which we can modify the PE word size, the number of PEs of the array, and the size of the memories.

For the current implementation, we obtained a maximum frequency of 67 MHz after constraining the design time requirements in the Quartus II tool to optimize the synthesis for speed instead of area. Further works will include pipelining the PE to achieve better performance in terms of clock frequency. Table 3 shows the synthesized configurations and their resource utilization.

7.2. Unaccelerated HMMER Performance. To measure the *hmmsearch* performance in a typical work environment

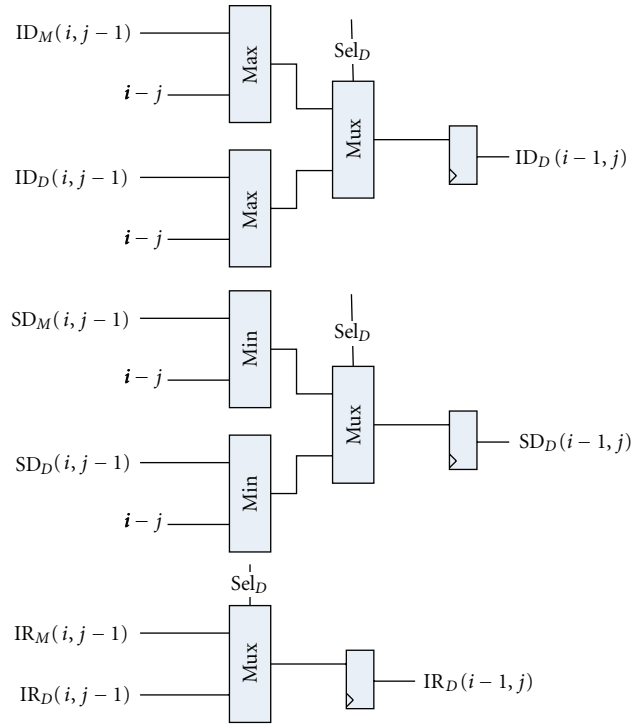

Figure 11: D state divergence calculating stage.

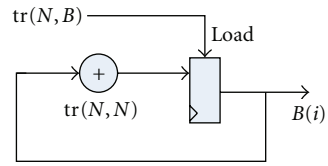

Figure 12: B score vector calculation unit (see Section 2).

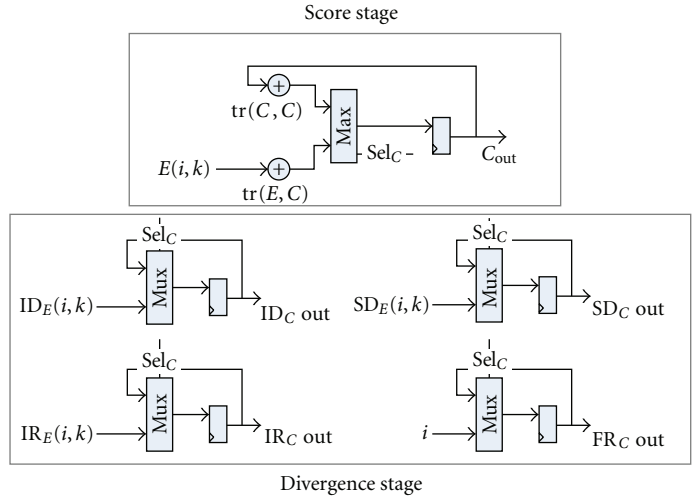

Figure 13: C vector calculation unit.

Table 3: Area and performance synthesis results.

NO. of PEs	Max. passes	Max. HMM nodes	Max. sequence size	Combinational ALUs	Dedicated registers	Memory bits	% Logic	Max. clock frequency (MHz)
25	25	625	8192	31738	18252	2609152	25	71
50	25	1250	8192	59750	35294	3121152	49	71
75	25	1875	8192	93132	52520	3663152	75	69
85	27	2295	8192	103940	59285	5230592	84	67

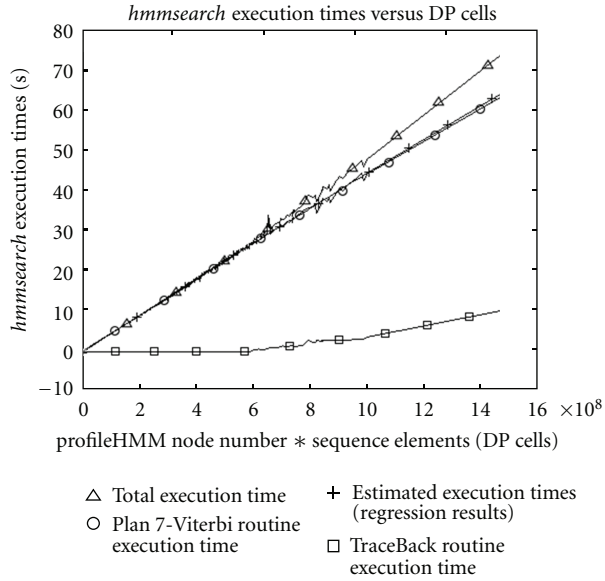

Figure 14: Unaccelerated *hmmsearch* performance for the test set.

we used a platform composed of an Intel Centrino Duo processor running at 1.8 GHz, 4 GB of RAM memory, and a 250 GB hard drive. HMMER was compiled to optimize execution time inside a Kubuntu Linux distribution. We also modified the *hmmsearch* program in order to obtain the execution times only for the Viterbi algorithm, as it was our main target for acceleration.

The characterization of HMMER was done by executing the entire set of tests (4 sets of 2000 randomly sampled sequences compared against 10340 profile HMMs) in the modified *hmmsearch* program. This was done to obtain an exact measure of the execution times of the unaccelerated software and to make its characterization when executing in our test platform. Figure 14 shows the obtained results for the experiments.

The line with triangular markers represents the total execution time of the *hmmsearch* program including the alignment generation times, the line with circular markers represents the execution time only for the Viterbi algorithm, the line with square markers represents the time consumed by the program when generating the alignments, and the line with the plus sign markers corresponds to the expected execution times obtained via the characterization expression shown in (8).

Let l_i be the number of amino acids in sequence S_i and let m_j be the number of nodes in the profile HMM P_j. Then the time to make the comparison between the profile HMM and the query sequence ($t_{s(i,j)}$) was found to be accurately represented by (8) which was found by making a least-squares regression on the data plotted in the circle-marked line of Figure 14:

$$t_{s(i,j)} \longleftarrow -1.3684 * 10^{-18}\left(m_j l_i\right)^2 + 4.3208 * 10^{-8} * \left(m_j l_i\right) - 0.1160. \tag{8}$$

Even though we ran our tests with all the profile HMMs in the PFam-A database [2], we chose to show results only for 6 representative profile HMMs that include the smallest and the largest of the database, due to space limitations. Table 4 shows the estimated execution time obtained with (8) and its error percentage when compared to the actually measured execution times. We can calculate the number of average cell updates per second (CUPS) as the total number of elements of the entire data set sequences times the number of nodes of the profiles in the set divided by the complete execution time of the processing. We obtained a performance of 23.157 mega-CUPS for HMMER executing on the test platform.

7.3. Hardware Performance. We formulated an equation for performance prediction of the proposed accelerator, taking into account the possible delays, including systolic array data filling and consuming, profile HMM probabilities loading into RAM memories, and probability reloading delays when switching between passes. In order to validate the equation's results, we developed a test bench to execute all the test sets. I/O data transmission delays from/to the PC host were not considered into the formula due to the fact that, in platforms such as the XD2000i [23], data transmission rates are well above the maximum required for the system (130 MBps).

Let m_i be the number of nodes of the current HMM, S_j the size of the current query sequence being processed, n the number of PEs in hardware, f the maximum system frequency, T_{hw} the throughput of the system (measured in CUPS), and $t_{h(i,j)}$ the time the accelerator takes to process one sequence set. Then T_{hw} and $t_{h(i,j)}$ are fully described by (9) and (10), where $25n\lceil m_i/n\rceil$ are the number of cycles spent loading the current HMM into memory, n are the array filling number of cycles, $(S_j + 6)\lceil m_i/n\rceil$ are the cycles spent while processing the current sequence, 3 are the cycles spent loading the special transitions, and $S_j m_i$ are number of cells

Table 4: Modified *hmmsearch* performance results.

Sequence set elements	Number of HMM nodes	Measured time (total)	Measured time (Viterbi only)	Estimated time (Viterbi only)	Error (%)
687406	788	23.40	23.28	22.871	1.75
	10	0.40	0.35	0.1810	48.2
	226	6.55	6.47	6.5635	1.42
	337	9.85	9.8	9.8199	0.2
	2295	74.49	64.09	64.6425	0.8
	901	26.32	26.25	26.1199	0.4
697407	788	24.34	23.48	23.2158	1.12
	10	0.47	0.41	0.1853	54.1
	226	6.68	6.66	6.6602	0.003
	337	9.88	9.83	9.9634	1.35
	2295	78.87	62.89	65.5334	4.2
	901	27.55	25.96	26.4938	2.05
700218	788	24.40	23.37	23.3082	0.264
	10	0.42	0.38	0.1865	50.92
	226	6.76	6.72	6.6873	0.486
	337	10.26	9.84	10.0037	1.663
	2295	81.23	62.25	65.7849	5.678
	901	27.41	26.33	26.5989	1.021
712734	788	25.42	24.03	23.7193	1.293
	10	0.42	0.37	0.1919	48.13
	226	6.82	6.77	6.8083	0.565
	337	10.09	10.01	10.1832	1.730
	2295	81.07	63.81	66.8985	4.840
	901	27.46	26.82	27.0665	0.919

* Execution times are all expressed in seconds.

that the unaccelerated algorithm will have to calculate to process the current sequence with the current HMM:

$$T_{hw} = \frac{\sum_{i=1}^{\#\text{Seqs}} \sum_{j=1}^{\#\text{HMMs}} S_i m_j}{\sum_{j=1}^{\#\text{HMMs}} \left[\left(\sum_{i=1}^{\#\text{Seqs}} (S_i + 6) \left\lceil m_j/n \right\rceil \right) + 25n \left\lceil m_j/n \right\rceil + n - 2 \right]} * f, \tag{9}$$

$$t_{h(i,j)} = \frac{(S_i + 6) \left\lceil m_j/n \right\rceil + 25n \left\lceil m_j/n \right\rceil + n - 2}{f}. \tag{10}$$

We made the performance evaluation for the 4 proposed systolic PE arrays (25, 50, 75, and 85 PEs) and found out that the two characteristics that greatly influence the performance of the array are the quantity of PEs implemented in the array and the number of nodes of the profile HMM we are comparing the sequences against.

Table 5 shows the obtained performances for all the array variations when executing the comparisons for our 4 sets of sequences against the 6 profile HMM subsets. The best result for each case is shown in bold. From the table we can see that performance increases significantly with the number of implemented PEs. Also we can observe that the system has better performance for profile HMMs whose node number is an exact multiple of the array node number. This is due to the fact that, when a PE does not correspond to a node inside the profile HMM, its transition and emission probabilities are set to minus infinity in order to stop that PE to modify the previously calculated result and only forward that result, thus wasting a clock cycle and affecting performance.

Figures 15 and 16 show the variations in the accelerator performance with the implemented PE number and the profile HMM node number, as seen from the experimental results.

From Figure 16 we can see that, as the performance varies according with profile HMM node number, there is an envelope curve around the performance data which shows the maximum and minimum performances of the array when varying the number of the HMM nodes.

7.4. Reprocessing Stage Performance (with Plan7-Viterbi-DA). When aligning different sequences with profile HMMs it is unlikely to find two alignments that are equal. Due to this fact, we cannot predict beforehand what will be the performance of the reprocessing stage as the divergence limits for every alignment are likely to be different. To make

Table 5: Hardware performance results.

Sequence set elements	Number of HMM nodes	25 PEs		50 PEs		75 PEs		85 PEs	
		T_{hw} (GCUPS)	t_h (sec)	T_{hw} (GCUPS)	t_h (sec)	T_{hw} (GCUPS)	t_h (sec)	T_{hw} (GCUPS)	t_h (sec)
687406	788	1.7468	0.3101	3.4903	0.1552	4.9293	0.1068	5.4203	0.0971
	10	0.7093	0.0097	0.7086	0.0097	0.6880	0.0097	0.6877	0.0097
	226	1.6031	0.0969	3.2033	0.0485	3.8876	0.0388	5.1815	0.0291
	337	1.7075	0.1357	3.4118	0.0679	4.6377	0.0485	5.7949	0.0388
	2295	**1.7695**	0.8915	**3.5358**	0.4462	**5.0942**	0.3010	**5.8468**	0.2622
	901	1.7274	0.3586	3.3607	0.1843	4.7691	0.1262	5.6341	0.1068
697407	788	1.7468	0.3146	3.4904	0.1574	4.9295	0.1083	5.4205	0.0985
	10	0.7093	0.0098	0.7086	0.0098	0.6880	0.0099	0.6877	0.0099
	226	1.6031	0.0983	3.2033	0.0492	3.8878	0.0394	5.1817	0.0296
	337	1.7075	0.1376	3.4119	0.0689	4.6379	0.0492	5.7952	0.0394
	2295	**1.7695**	0.9045	**3.5359**	0.4527	**5.0944**	0.3053	**5.8471**	0.2660
	901	1.7274	0.3638	3.3608	0.1870	4.7693	0.1280	5.6344	0.1084
700218	788	1.7468	0.3159	3.4905	0.1581	4.9296	0.1088	5.4206	0.0989
	10	0.7093	0.0099	0.7086	0.0099	0.6880	0.0099	0.6877	0.0099
	226	1.6031	0.0987	3.2034	0.0494	3.8878	0.0396	5.1818	0.0297
	337	1.7075	0.1382	3.4120	0.0692	4.6379	0.0494	5.7953	0.0396
	2295	**1.7695**	0.9081	**3.5359**	0.4545	**5.0945**	0.3066	**5.8472**	0.2671
	901	1.7274	0.3652	3.3608	0.1877	4.7693	0.1286	5.6345	0.1088
712734	788	1.7468	0.3215	3.4906	0.1609	4.9298	0.1107	5.4209	0.1007
	10	0.7093	0.0100	0.7086	0.0101	0.6880	0.0101	0.6878	0.0101
	226	1.6031	0.1005	3.2035	0.0503	3.8880	0.0403	5.1821	0.0302
	337	1.7075	0.1407	3.4121	0.0704	4.6382	0.0503	5.7956	0.0403
	2295	**1.7695**	0.9244	**3.5360**	0.4626	**5.0947**	0.3120	**5.8475**	0.2719
	901	1.7274	0.3718	3.3609	0.1911	4.7696	0.1308	5.6348	0.1108

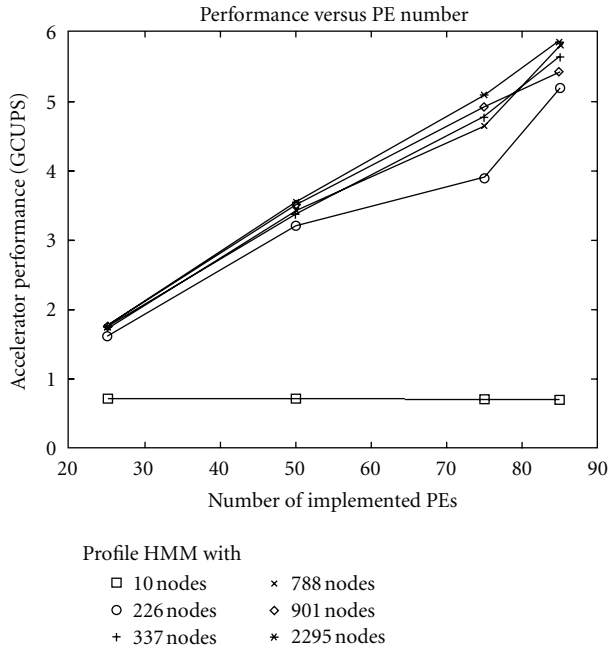

Figure 15: Performance versus number of PEs relation.

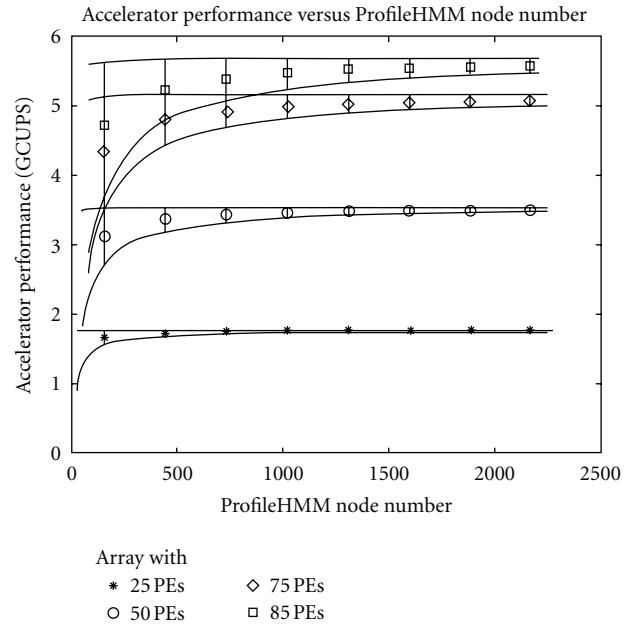

Figure 16: Performance versus number of HMM nodes envelope curves.

Table 6: Second-stage performance estimations.

Sequence set elements	Number of HMM nodes	Entire sequence set processing time in unaccelerated HMMER (sec)	Significant sequences reprocessing time with prefilter and unaccelerated HMMER (sec)	Divergence accelerated significant sequences reprocessing time (sec)
687406	788	23.40	0.234	0.0515
	10	0.40	0.004	0.0009
	226	6.55	0.0655	0.0144
	337	9.85	0.0985	0.0217
	2295	74.49	0.7449	0.1639
	901	26.32	0.2632	0.0579
697407	788	24.34	0.2434	0.0535
	10	0.47	0.0047	0.001
	226	6.68	0.0668	0.0147
	337	9.88	0.0988	0.0217
	2295	78.87	0.7887	0.1735
	901	27.55	0.2755	0.0606
700218	788	24.40	0.244	0.0537
	10	0.42	0.0042	0.0009
	226	6.76	0.0676	0.0149
	337	10.26	0.1026	0.0226
	2295	81.23	0.8123	0.1787
	901	27.41	0.2741	0.0603
712734	788	25.42	0.2542	0.0559
	10	0.42	0.0042	0.0009
	226	6.82	0.0682	0.015
	337	10.09	0.1009	0.0222
	2295	81.07	0.8107	0.1784
	901	27.46	0.2746	0.0604

an estimate of the performance of the second stage, we made a study in which we executed the comparison of the 20 top profile HMMs from the PFam-A [2] database with our 4 sets of query sequences to obtain both the similarity score and the divergence data for them. Then we built a graph plotting the similarity score threshold and the number of sequences with a similarity score greater than the threshold. From this graph we learned that less than 1% of the sequences were considered significant, even relaxing the threshold to include very bad alignments. With this information, we plotted the percentage of the DP matrices that the second stage of the system will have to reprocess in order to find out the worst case situation and make our estimations based on it. From Figure 17 we can see that, for the experimental data considered, in the worst case the divergence region only corresponds to 22% of the DP matrices.

To obtain the second-stage performance estimations for HMMER ($t_{\text{rep}(i,j)}$ in (6)), we obtained the percentage of significant sequences (p_s), multiplied it by the worst case percentage of the DP matrices that the second stage has to reprocess in order to generate the alignment (p_c), and then we multiplied it by the time the program *hmmsearch* takes to do the whole query sequence (S_i) comparison with a profile HMM (P_j). Equation (8) shows the expression used to estimate the performance for the second stage. Table 6 presents the obtained results and also shows the comparison between the times the second stage will spend reprocessing the significant sequences with and without the Plan7-Viterbi-DA. As shown in Table 6, we obtained a performance gain up to 5 times only in the reprocessing stage.

$$t_{(\text{reg}(i,j))} = t * p_s * p_c \tag{11}$$

7.5. Total System Performance. In Section 6, we proposed two approaches to evaluate the performance for the system. For the first approach based in CUPS, we obtained a maximum system performance of up to 5.8 GCUPS when implementing a system composed by 85 PEs. This gives us a maximum gain of 254 times over the performance of unaccelerated HMMER software. For the second approach, as we obtained the individual processing times for every stage of the execution, we can determine the overall system performance by applying (6) to the results obtained in Tables 5 and 6. When including the Plan7-Viterbi divergence reprocessing stage, we got a maximum gain of up to 182 times the unaccelerated software, which still means a significant gain when comparing to unaccelerated HMMER. Table 7 presents the total execution time of the system and

Table 7: Total system performance and obtained performance gains.

Sequence set elements	Number of HMM nodes	Prefilter hardware execution time (sec)	Divergence second-stage execution time (sec)	Total time ($t_{sa(i,j)}$)	Unaccelerated HMMER execution time (sec)	Obtained gain
687406	788	0.0971	0.0515	0.1486	23.40	157.4697
	10	0.0097	0.0009	0.0106	0.40	37.7358
	226	0.0291	0.0144	0.0435	6.55	150.5747
	337	0.0388	0.0217	0.0605	9.85	162.8099
	2295	0.2622	0.1639	0.4261	74.49	**174.8181**
	901	0.1068	0.0579	0.1647	26.32	159.8057
697407	788	0.0985	0.0535	0.152	24.34	160.1316
	10	0.0099	0.001	0.0109	0.47	43.1193
	226	0.0296	0.0147	0.0443	6.68	150.7901
	337	0.0394	0.0217	0.0611	9.88	161.7021
	2295	0.2660	0.1735	0.4395	78.87	**179.4539**
	901	0.1084	0.0606	0.169	27.55	163.0178
700218	788	0.0989	0.0537	0.1526	24.40	159.8952
	10	0.0099	0.0009	0.0108	0.42	38.8889
	226	0.0297	0.0149	0.0446	6.76	151.5695
	337	0.0396	0.0226	0.0622	10.26	164.9518
	2295	0.2671	0.1787	0.4458	81.23	**182.2118**
	901	0.1088	0.0603	0.1691	27.41	162.0934
712734	788	0.1007	0.0559	0.1566	25.42	162.3244
	10	0.0101	0.0009	0.011	0.42	38.1818
	226	0.0302	0.015	0.0452	6.82	150.885
	337	0.0403	0.0222	0.0625	10.09	161.44
	2295	0.2719	0.1784	0.4503	81.07	**180.0355**
	901	0.1108	0.0604	0.1712	27.46	160.3972

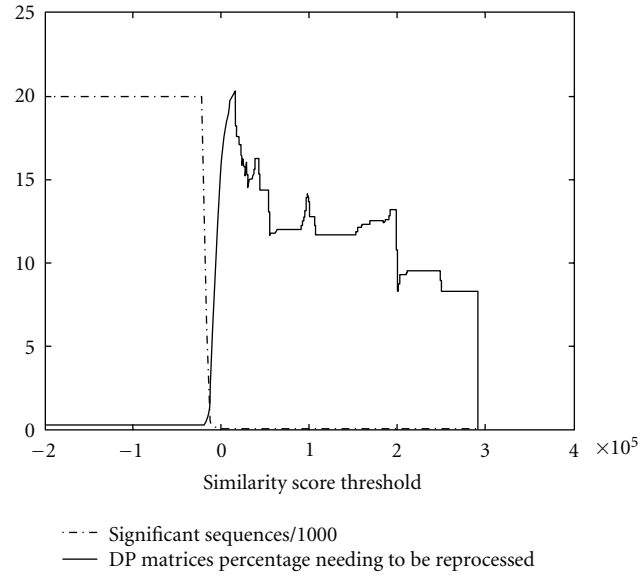

Figure 17: Number of significant sequences and DP percentage that is required to reprocess in software versus similarity score threshold.

Table 8: Related work and comparison with our solution.

Reference	Number of PEs	Max. number of HMM nodes	Max. sequence size	Complete Plan7-Viterbi algorithm	Clock (MHz)	Performance (GCUPS)	Gain	FPGA
[3]	68	544	1024	*N*	180	10	190	Xilinx Virtex II 6000
[13]	90	1440	1024	*N*	100	9	247	Xilinx 2VP100
[11]	50	—	—	*N*	200	5 to 20	—	Not Synthesized
[14]	72	1440	8192	*N*	74	3.95	195	XC2V6000
[15]	10	256	—	*Y*	70	7	300	XC3S1500
[16]	50	—	—	*N*	66	1.3	50	Xilinx Spartan 3 4000
[20]	25	—	—	*Y*	130	3.2	56.8	Xilinx Virtex 5 110-T
Our work	**85**	**2295**	**8192**	*N*	**67**	**5.8**	**254 (182*)**	**Altera Stratix II EP2S180F1508C3**

* Including significant sequences reprocessing times.

shows the obtained performance gains. The table presents a summary of the execution time for each individual part of the system and calculates the performance gains with respect to the unaccelerated HMMER by applying (6).

Table 8 shows a brief comparison of this work with the ones found in the literature. We support longest test sequences and bigger profiles when compared with most works. As we include the divergence stage, we have to pay an area penalty, which limit the maximum number of PEs when compared with [13] and can affect the performance of the system. Nevertheless, we obtain additional gains from the divergence, a fact that justify the area overhead. Our architecture performs worse than complete Viterbi implementations such as the one presented in [15], but these cases are uncommon, and even if we relax the threshold for a sequence to be considered significant, the inclusion of the accelerator yields significant speedup.

8. Conclusions

In this paper, we introduced the Plan7-Viterbi-DA that enables the implementation of a hardware accelerator for the *hmmsearch* and *hmmpfam* programs of the HMMER suite. We proposed an accelerator architecture which acts as a pre-filtering phase and uses the Plan7-Viterbi-DA to avoid the full reprocessing of the sequence in software. We also introduced a more accurate performance measurement strategy when evaluating HMMER hardware accelerators, which not only includes the time spent on the pre-filtering phase or the hardware throughput but also includes reprocessing times for the significant sequences found in the process.

We implemented our accelerator in VHDL, obtaining performance gains of up to 182 times the performance of the HMMER software. We also made a comparison of the present work with those found in the literature and found that, despite the increased area, we managed to fit a considerable amount of PEs inside the FPGA, which are capable of comparing query sequences with even the largest profile HMM present in the PFam-A database.

For future works we intend to adapt the Plan7-Viterbi-DA to a complete version of the Plan7-Viterbi algorithm (including the *J* state) and make a pipelined version of the PE architecture, in order to further increase the performance gains achieved when integrating the array with the HMMER software.

Acknowledgments

The authors would like to acknowledge the CNPq, the National Microelectronics Program (PNM), the FINEP, the Brazilian Millennium Institute (NAMITEC), the CAPES, and the Fundect-MS for funding this work.

References

[1] The Universal Protein Resource—UniProt, June 2009, http://www.uniprot.org/.

[2] Sanger's Institute PFAM Protein Sequence Database, May 2009, http://pfam.sanger.ac.uk/.

[3] A. C. Jacob, J. M. Lancaster, J. D. Buhler, and R. D. Chamberlain, "Preliminary results in accelerating profile HMM search on FPGAs," in *Proceedings of the 21st International Parallel and Distributed Processing Symposium, (IPDPS '07)*, Long Beach, Calif, USA, March 2007.

[4] "HMMER: biosequence analysis using profile hidden Markov models," 2006, http://hmmer.janelia.org/.

[5] R. Durbin, S. Eddy, A. Krogh, and G. Mitchison, *Biological Sequence Analysis Probabilistic Models of Proteins and Nucleic Acids*, Cambridge University Press, New York, NY, USA, 2008.

[6] R. Darole, J. P. Walters, and V. Chaudhary, "Improving MPI-HMMER's scalability with parallel I/O," Tech. Rep. 2008-11, Department of Computer Science and Engineering, University of Buffalo, Buffalo, NY, USA, 2008.

[7] G. Chukkapalli, C. Guda, and S. Subramaniam, "SledgeHMMER: a web server for batch searching the Pfam database," *Nucleic Acids Research*, vol. 32, supplement 2, pp. W542–W544, 2004.

[8] "HMMER on the sun grid project," July 2009, http://www.psc.edu/general/software/packages/hmmer/.

[9] D. R. Horn, M. Houston, and P. Hanrahan, "ClawHMMER: a streaming HMMer-search implementation," in *Proceedings of the ACM/IEEE Supercomputing Conference, (SC '05)*, November 2005.

[10] GPU-HMMER, July 2009, http://www.mpihmmer.org/userguideGPUHMMER.htm.

[11] R. P. Maddimsetty, J. Buhler, R. D. Chamberlain, M. A. Franklin, and B. Harris, "Accelerator design for protein sequence HMM search," in *Proceedings of the 20th Annual International Conference on Supercomputing (ICS '06)*, pp. 288–296, New York, NY, USA, July 2006.

[12] "BLAST: Basic Local Alignment Search Tool," September 2009, http://blast.ncbi.nlm.nih.gov/.

[13] K. Benkrid, P. Velentzas, and S. Kasap, "A high performance reconfigurable core for motif searching using profile HMM," in *Procedings of the NASA/ESA Conference on Adaptive Hardware and Systems (AHS '08)*, pp. 285–292, Noordwijk, The Netherlands, June 2008.

[14] T. F. Oliver, B. Schmidt, Y. Jakop, and D. L. Maskell, "High speed biological sequence analysis with hidden Markov models on reconfigurable platforms," *IEEE Transactions on Information Technology in Biomedicine*, vol. 13, no. 5, pp. 740–746, 2009.

[15] J. P. Walters, X. Meng, V. Chaudhary et al., "MPI-HMMER-boost: distributed FPGA acceleration," *Journal of VLSI Signal Processing Systems*, vol. 48, no. 3, pp. 223–238, 2007.

[16] S. Derrien and P. Quinton, "Parallelizing HMMER for hardware acceleration on FPGAs," in *Proceedings of the International Conference on Application-specific Systems, Architectures and Processors (ASAP '07)*, pp. 10–17, Montreal, Canada, July 2007.

[17] L. Hunter, *Artificial Intelligence and Molecular Biology*, MIT Press, 1st edition, 1993.

[18] D. Gusfield, *Algorithms on Strings, Trees and Sequences: Computer Science and Computational Biology*, Cambridge University Press, 1997.

[19] L. R. Rabiner, "A tutorial on hidden Markov models and selected applications in speech recognition," *Proceedings of the IEEE*, vol. 77, no. 2, pp. 257–286, 1989.

[20] Y. Sun, P. Li, G. Gu et al., "HMMer acceleration using systolic array based reconfigurable architecture," in *Proceedings of the ACM/SIGDA International Symposium on Field Programmable Gate Arrays (FPGA '09)*, p. 282, New York, NY, USA, May 2009.

[21] T. Takagi and T. Maruyama, "Accelerating hmmer search using FPGA," in *Proceedings of the19th International Conference on Field Programmable Logic and Applications (FPL '09)*, pp. 332–337, Prague Czech Republic, September 2009.

[22] R. B. Batista, A. Boukerche, and A. C. M. A. de Melo, "A parallel strategy for biological sequence alignment in restricted memory space," *Journal of Parallel and Distributed Computing*, vol. 68, no. 4, pp. 548–561, 2008.

[23] XtremeData Inc., July 2009, http://www.xtremedata.com/.